



Light-Controlled Affinity Purification of Protein Complexes Exemplified by the Resting ZAP70 Interactome

Maximilian Hörner^{1,2,3†}, Julian Eble^{1,2†}, O. Sascha Yousefi^{1,2,3†}, Jennifer Schwarz^{1,3†}, Bettina Warscheid^{1,2,3}, Wilfried Weber^{1,2,3*} and Wolfgang W. A. Schamel^{1,2,3,4*}

¹ Faculty of Biology, University of Freiburg, Freiburg, Germany, ² Signalling Research Centres BIOSS and CIBSS, University of Freiburg, Freiburg, Germany, ³ Spemann Graduate School of Biology and Medicine, University of Freiburg, Freiburg, Germany, ⁴ Centre for Chronic Immunodeficiency CCI, Medical Center, University of Freiburg, Freiburg, Germany

OPEN ACCESS

Edited by:

Jorge Bernardino De La Serna,
United Kingdom Research and
Innovation, United Kingdom

Reviewed by:

Gottfried Baier,
Innsbruck Medical University, Austria
Cosima T. Baldari,
University of Siena, Italy

*Correspondence:

Wilfried Weber
wilfried.weber@biologie.uni-freiburg.de
Wolfgang W. A. Schamel
wolfgang.schamel@
biologie.uni-freiburg.de

[†]These authors have contributed
equally to this work

Specialty section:

This article was submitted to
T Cell Biology,
a section of the journal
Frontiers in Immunology

Received: 21 December 2018

Accepted: 28 January 2019

Published: 26 February 2019

Citation:

Hörner M, Eble J, Yousefi OS,
Schwarz J, Warscheid B, Weber W
and Schamel WWA (2019)
Light-Controlled Affinity Purification of
Protein Complexes Exemplified by the
Resting ZAP70 Interactome.
Front. Immunol. 10:226.
doi: 10.3389/fimmu.2019.00226

Multiprotein complexes control the behavior of cells, such as of lymphocytes of the immune system. Methods to affinity purify protein complexes and to determine their interactome by mass spectrometry are thus widely used. One drawback of these methods is the presence of false positives. In fact, the elution of the protein of interest (POI) is achieved by changing the biochemical properties of the buffer, so that unspecifically bound proteins (the false positives) may also elute. Here, we developed an optogenetics-derived and light-controlled affinity purification method based on the light-regulated reversible protein interaction between phytochrome B (PhyB) and its phytochrome interacting factor 6 (PIF6). We engineered a truncated variant of PIF6 comprising only 22 amino acids that can be genetically fused to the POI as an affinity tag. Thereby the POI can be purified with PhyB-functionalized resin material using 660 nm light for binding and washing, and 740 nm light for elution. Far-red light-induced elution is effective but very mild as the same buffer is used for the wash and elution. As proof-of-concept, we expressed PIF-tagged variants of the tyrosine kinase ZAP70 in ZAP70-deficient Jurkat T cells, purified ZAP70 and associating proteins using our light-controlled system, and identified the interaction partners by quantitative mass spectrometry. Using unstimulated T cells, we were able to detect the known interaction partners, and could filter out all other proteins.

Keywords: optogenetics, affinity purification, phytochrome, ZAP70, protein-protein interaction, mass spectrometry

INTRODUCTION

Most, if not all, biochemical processes in cells, such as signal transduction, rely on protein-protein-interactions (1, 2). In the cells of the immune system for example, signalosomes change in their composition upon stimulation of cell surface receptors (3, 4). A well-studied example is the binding of the T cell antigen receptor (TCR) complex to the tyrosine kinase ZAP70 in resting T cells (5–8). Upon ligand binding to the TCR, ZAP70 gets activated by phosphorylation and detaches from the TCR (9) leading to the generation of new intracellular interactions and the remodeling of signalosomes (10). As those protein-protein-interactions control cell behavior, their investigation is of key interest in immunological and biological research.

Interaction partners of proteins are usually identified by purification of a protein of interest (POI) and analyzing the co-purified proteins by mass spectrometry (11, 12). Besides the use of POI-specific antibodies, one common approach is the purification of the POI via an affinity tag. There, the POI is expressed as a fusion protein with an affinity tag that binds specifically to a resin material. Then the cells expressing the fusion protein are lysed with a detergent, insoluble material is removed by centrifugation, and the lysate is added to the resin. Subsequently, the POI together with its interacting proteins binds to the resin. After washing, the POI together with its interaction partners can be eluted from the resin, e.g., by a change in the pH (FLAG tag, HA tag), ion concentration (Poly-Arg tag), temperature (protein G tag), or by addition of metal chelators (CBP tag) or molecules that compete with the binding of the affinity tag to the resin (Strep tag, SBP tag, Poly-His tag) (13, 14). Alternatively, the affinity tag is linked to the POI using a sequence that can be cleaved by a protease, such as Tobacco Etch Virus (TEV) protease (15). Hence, elution is achieved by adding the protease, cleaving the POI off the resin. Importantly, all the different approaches have in common that the changed biochemical environment in the elution step can also result in the release of unspecifically bound proteins from the resin material resulting in false positive hits in the following analysis. One approach to reduce the number of contaminants in the eluate is the sequential usage of two different affinity tags, named tandem affinity purification (TAP) (16). However, due to the thereby prolonged time needed for purification, more transient and weak interactors may be lost during this procedure.

In this study, we address this problem by developing an optogenetics-based purification approach allowing elution of tagged proteins by simply changing the wavelength of light with which the resin is illuminated. Thus, all biochemical parameters, such as the ones mentioned above, stay constant, minimizing the elution of proteins that were bound to the resin and not to the POI. We made use of the light-dependent protein-protein interaction between phytochrome B (PhyB) and its phytochrome interacting factor 6 (PIF6) both from *Arabidopsis thaliana* (17). Upon illumination with 660 nm red light PhyB switches to its Pfr conformational state (PhyB far-red absorbing state) in which it interacts with PIF6 with a nanomolar affinity (18). With 740 nm far-red light PhyB undergoes a conformational transition to the Pr state (PhyB red absorbing state) preventing binding to PIF6. This light-dependent protein-protein interaction was applied for several optogenetic applications (19), such as the control of protein or organelle localization (18, 20), signaling (21), nuclear transport of proteins (22), or gene expression (23).

Here, we make the red light-dependent interaction between PhyB and PIF6 applicable to the affinity purification of protein complexes. To this end, we identified a truncated variant of PIF6 comprising only 22 amino acids that reversibly interacts with PhyB and therefore can be used as an affinity tag for the POI. After characterization of the key parameters of our light-controlled affinity purification approach, we applied our method for the identification of interaction partners of ZAP70 in resting T cells by quantitative mass spectrometry.

RESULTS AND DISCUSSION

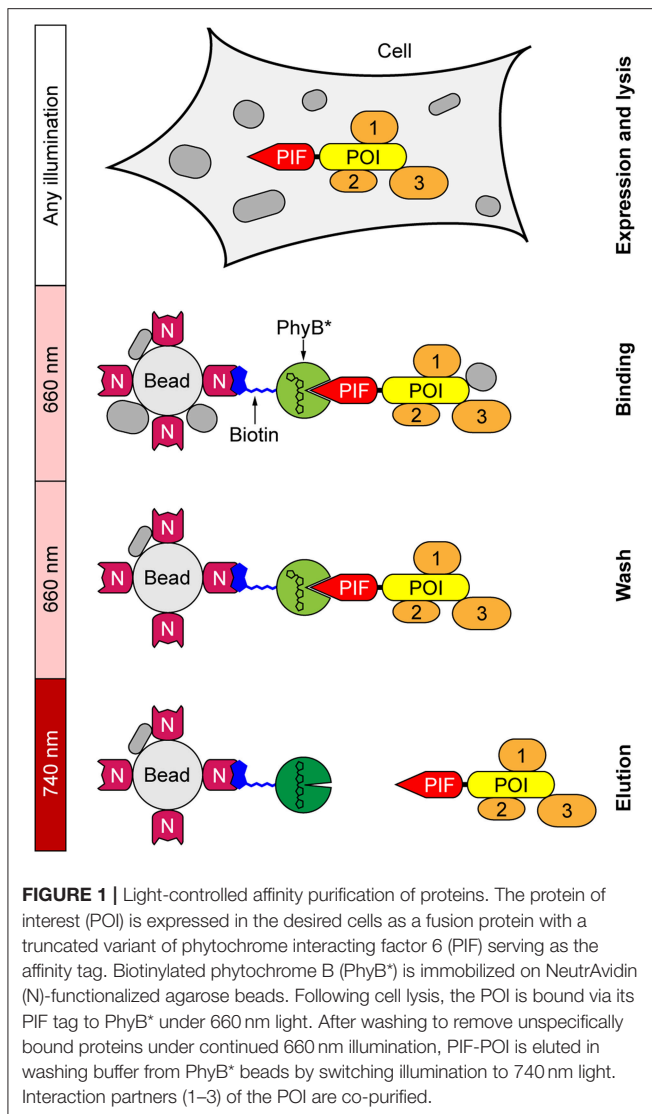
In our new light-controlled affinity purification approach, a fusion protein between the POI and a truncated version of PIF6 is expressed in the desired cells (**Figure 1**). After cell lysis, the lysate is loaded under 660 nm light illumination onto agarose beads that have been functionalized with PhyB. Illumination with 660 nm light switches PhyB into the Pfr state, thus immobilizing the PIF-POI fusion protein and potential interaction partners to the PhyB beads. Afterwards the beads are washed under continued 660 nm illumination for removal of unspecific bound proteins. Finally, PIF-POI and its binding partners are eluted in the same buffer as used in the washing steps by simply changing illumination to 740 nm light, as light of this wavelength switches PhyB into the Pr state that terminates the interaction with PIF.

PhyB*-Functionalized Resin Material

In order to functionalize agarose beads with PhyB, we used a biotinylated and hexahistidine-tagged variant of PhyB comprising amino acids 1-651 (24). This protein was produced together with the enzymes for the biosynthesis of the required chromophore phycocyanobilin (PCB) in *E. coli*. We purified this PhyB variant (designated as PhyB*) via immobilized metal ion affinity chromatography and quantified its biotinylation by binding of the protein to NeutrAvidin-functionalized agarose beads. Using an excess of beads, we observed that ~98% of PhyB* was biotinylated (**Supplementary Figure 1**). To determine the PhyB* binding capacity of the NeutrAvidin agarose beads, we incubated a fixed amount of beads with increasing amounts of PhyB* and monitored a decrease in the ratio of beads-bound PhyB* (**Supplementary Figure 1**). Saturation of the beads was reached with approximately 0.2 nmol PhyB* per 1 μ l beads. In the following, 1 μ l NeutrAvidin beads were always incubated with ~0.27 nmol PhyB* resulting in a coupling of ~0.24 nmol PhyB* per 1 μ l of beads (~89% coupling efficiency, designated as PhyB* beads).

Truncation of the PIF6 Tag

It was shown that the N-terminal 100 amino acids of *A. thaliana* PIF6 [PIF6(1-100)] are sufficient for the reversible and light-dependent interaction with PhyB (17, 18). It is desirable to minimize the size of an affinity tag in order to disturb the fused POI as minimally as possible and to reduce undesired protein binding to the tag. Therefore, we aimed to further truncate PIF6(1-100) while maintaining its light-dependent interaction properties with PhyB. To this end, we performed a sequence alignment of different PIF variants from several plants to identify a region within the N-terminal 100 amino acids that is well-conserved and hence should constitute the core domain of PIF6 responsible for the light-dependent interaction with PhyB (**Supplementary Figure 2**). We found a conserved region between amino acids 15 and 36. Thus, we tested four different truncated PIF6 variants containing different amino acids within the 15–36 region and compared them to PIF6(1-100) (**Figure 2A**). To this end, we expressed the green fluorescent protein (GFP) fused to the selected PIF6 variants together with the untagged red fluorescent protein mCherry



in human embryonic kidney (HEK)-293T cells. Subsequently, PIF-tagged GFP was purified from the cell lysates with the PhyB*-functionalized beads and spin columns. During the purification process, we monitored the fluorescence of mCherry as a background control and of GFP as our POI (Figure 2B). We observed that all tested PIF tags allowed a light-controlled purification of the fused GFP. Remarkably, PIF6(15-33) and PIF6(15-36) showed a similar efficiency compared to PIF6(1-100). The amount of mCherry in the eluates was at least 4,000-fold reduced compared to the lysates, demonstrating the specificity of our purification protocol. Next, we compared our light-controlled purification approach with established affinity chromatography methods. These were based on the streptavidin binding peptide [SBP tag (25)] or on the TEV mediated cleavage of the POI from protein A [TEV_{CS}-ProteinA tag (26)]. We observed a similar recovery (70–80%, Supplementary Figure 3) and purity of the eluates (Figure 2C).

Characterization of the Purification Process

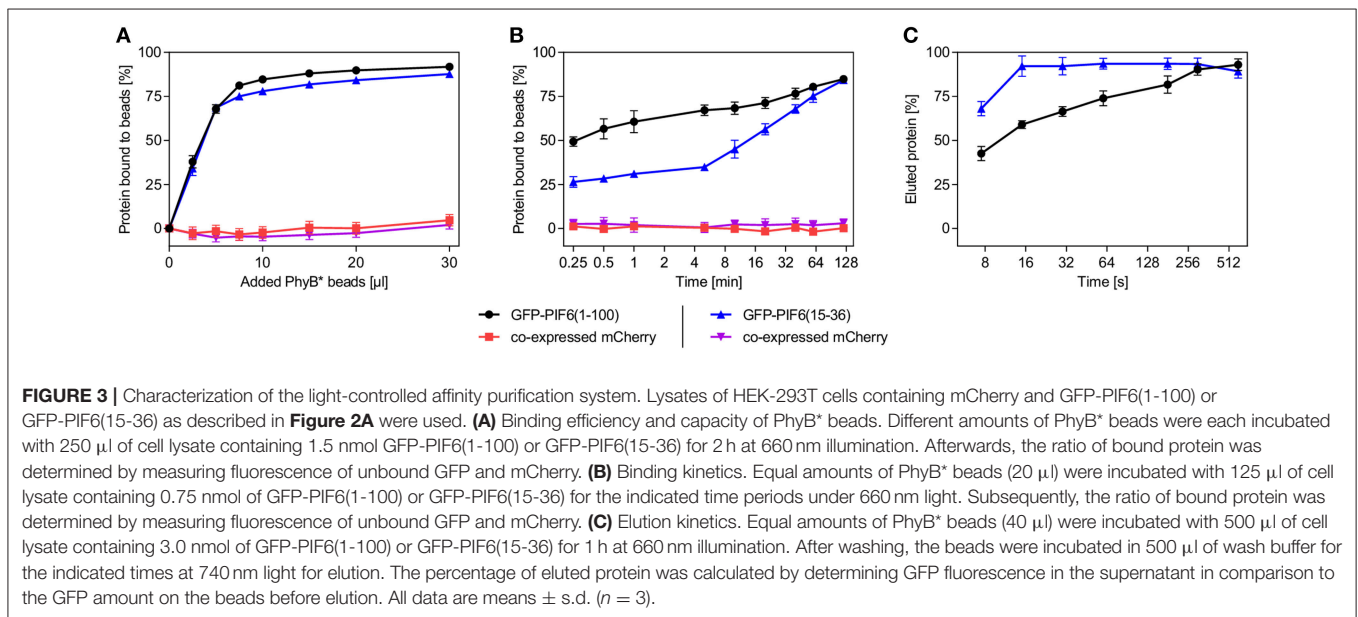
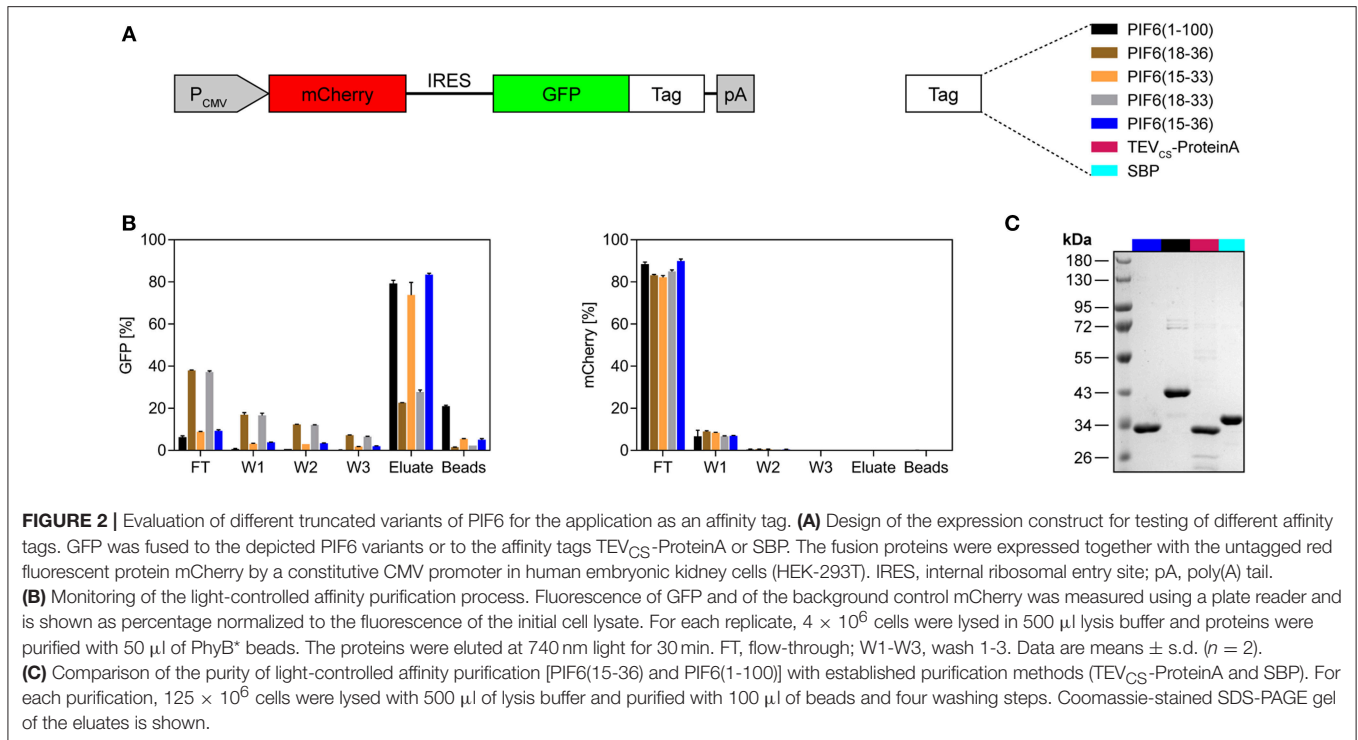
We characterized the purification process of GFP-PIF6(1-100) and GFP-PIF6(15-36) with PhyB* beads in more detail. We determined that within a binding period of 2 h at 660 nm illumination both PIF-tagged proteins were binding equally well to the PhyB* beads with a binding efficacy of ~85% (using an excess of PhyB* beads, Figure 3A). When the PIF-tagged proteins were in excess compared to PhyB*, ~0.21 nmol of GFP-PIF6(1-100) or GFP-PIF6(15-36) were binding per 1 μl of the PhyB* beads. We further observed that GFP-PIF6(1-100) was binding faster to the PhyB* beads under 660 nm light than GFP-PIF6(15-36) with 50% bound protein within 0.25 min compared to 15 min, respectively (Figure 3B). In contrast, GFP-PIF6(1-100) eluted slower from the PhyB* beads under 740 nm illumination than GFP-PIF6(15-36) with 80% released protein within 180 s compared to 16 s, respectively (Figure 3C).

Generation of ZAP70-PIF6 Tag Cell Lines

We tested our light-controlled purification approach for the identification of interaction partners of the kinase ZAP70 by quantitative mass spectrometry. ZAP70 is a central kinase involved in TCR signaling, which interacts with the components of the TCR such as CD3δ, CD3ε, CD3γ, or CD247 (5, 6, 10). We transduced the ZAP70-deficient Jurkat cell line P116 (27) with constructs expressing PIF6(1-100)- or PIF6(15-36)-tagged human ZAP70 and the fluorescent protein ZsGreen1 (Figure 4A). Based on the fluorescence of the marker ZsGreen1, we sorted transduced cells with low ZsGreen1 expression levels using flow cytometry to avoid overexpression of our ZAP70 fusion proteins. As expected, most of the sorted cells stably expressed ZsGreen1 as shown by flow cytometry (Figure 4B). Expression and correct size of the fusion proteins were confirmed by SDS-PAGE and Western Blotting using an anti-ZAP70 antibody (Figure 4C). Both tagged ZAP70 proteins were expressed to lower levels than endogenous ZAP70 in the Jurkat cell line. ZAP70 is directly downstream of the TCR, transducing TCR signals into the cell, such as Ca²⁺ influx into the cytosol. Indeed, when stimulating the TCR with anti-CD3 antibodies we detected a Ca²⁺ response in Jurkat cells, but not in P116 cells (Figure 4D). Moreover, the restored anti-CD3 induced Ca²⁺ influx in our stable cell lines showed that the fusion of the PIF tags to ZAP70 did not impair the functionality of ZAP70 (Figure 4D). The reduced Ca²⁺-flux in comparison to Jurkat cells can likely be attributed to the reduced expression level of our PIF-ZAP70 fusion constructs in comparison to the endogenous ZAP70 level of Jurkat cells (Figures 4C,D).

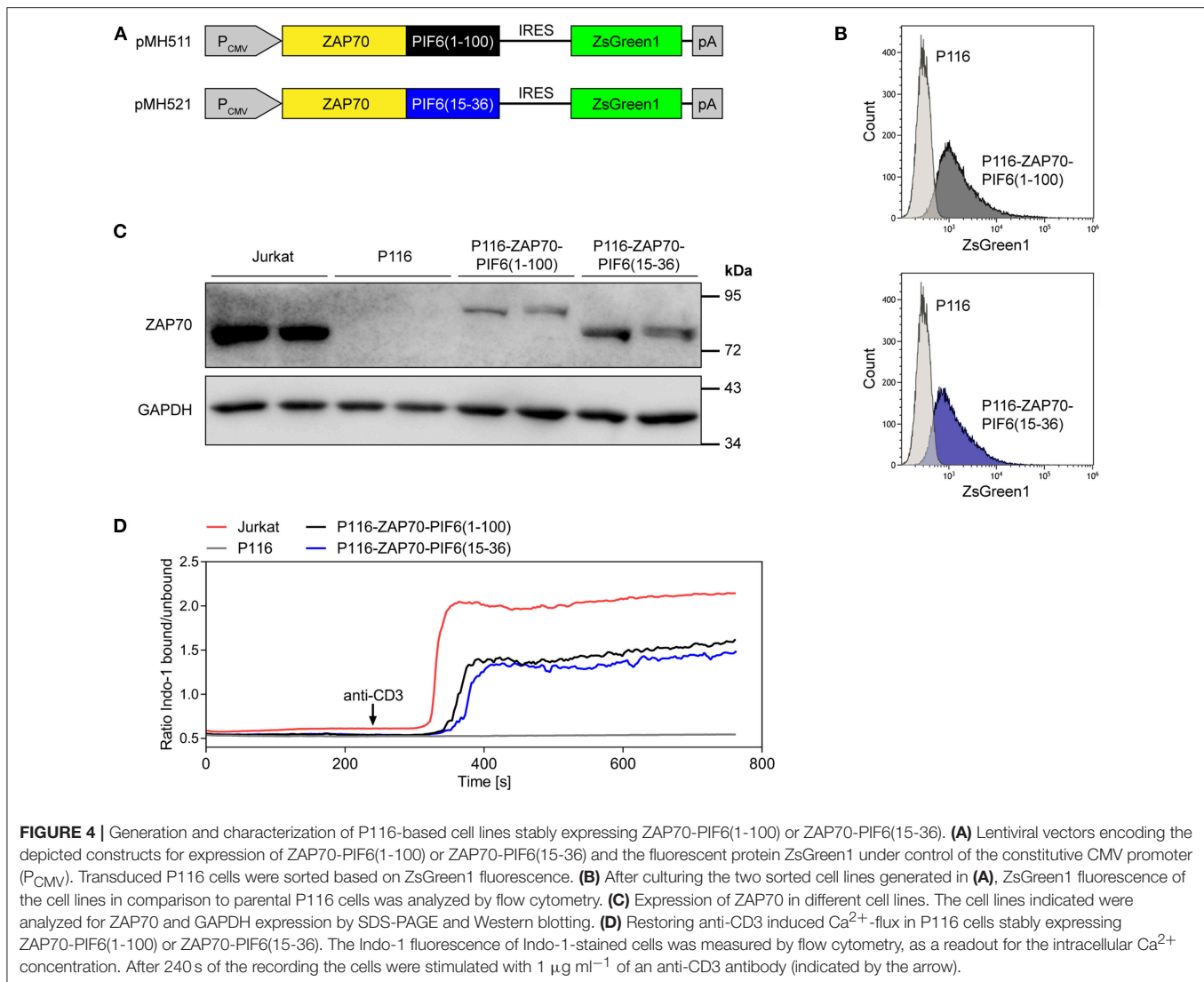
Identification of ZAP70 Interaction Partners by Mass Spectrometry

To test our new purification approach, we used both P116-derived stable cell lines in resting state, i.e., unstimulated. We purified PIF-tagged ZAP70 from these cell lines using our PhyB* beads and analyzed the cell lysates, the flow-throughs of the last washing step and the eluates by Western blotting against ZAP70 and GAPDH (Figure 5A). As a negative control, we performed



the same purification with Jurkat cells expressing non-tagged ZAP70. As expected, the eluates of the stable cell lines contained PIF-tagged ZAP70 of the correct molecular weight whereas the eluates of the Jurkat cells did not contain detectable amounts of ZAP70. The eluates of all purified cells showed a massive reduction in the GAPDH level compared to the cell lysates. This experiment demonstrates that we were able to specifically purify our POI, in this case ZAP70, using the new light-controlled affinity purification approach.

To validate whether we are able to identify interaction partners of ZAP70 by our light-controlled purification approach and whether we can eliminate false positives, we used the unstimulated P116 cells expressing PIF6(1-100)- or PIF6(15-36)-tagged human ZAP70. The usage of unstimulated cells has the following advantage. ZAP70 was shown to interact with the TCR in resting cells (7) thus this interaction serves as our positive control. Importantly, this ZAP70 is not phosphorylated on tyrosines (7). Since these tyrosines have to be phosphorylated



to serve as interactions sites for further signaling proteins (8), we do not expect any other interaction partners besides the TCR. Thus, we can assume that other proteins detected by mass spectrometry are false positives.

Next, we analyzed the eluates after 740 nm illumination and the flow-throughs of the last washing step of the above described unstimulated samples by mass spectrometry (3 biological replicates each, **Supplementary Table 1**). We first looked for proteins that were significantly enriched in the eluates derived from each ZAP70-PIF6 cell line compared to the eluates derived from the Jurkat cell line. We observed that for both ZAP70-PIF6 cell lines the 20 top hits ($p < 0.05$, sorted on protein enrichment) contained besides ZAP70 as the POI, the proteins CD247-i3 (i3, isoform 3), CD3D, CD3E, CD3G, and TRBC1/2 (**Figure 5B**). The different CD3 proteins, CD247 (also called CD3 ζ) as well as TRBC1/2 (also called TCR β chains) are all subunits of the TCR (28) which is known to associate with ZAP70 (5, 6, 29). As stated above, ZAP70 associates with the TCR in unstimulated primary T

cells (7) and most likely also in unstimulated Jurkat cells although to lower levels (30, 31). Since ZAP70 that is associated with the resting TCR is not phosphorylated (7) and thus might not have other binding partners, we conclude that the other proteins might be false positives. The two PIF6 tags showed a similar performance as shown by the high overlap of the 20 best hits (14 out of 20) and as visualized by the clustering of the proteins along the diagonal when plotting the enriched proteins against each other (**Figure 5C, Supplementary Table 2**). Together, this indicates that both PIF6(1-100) and PIF6(15-36) are suitable affinity tags that allow purification, and identification of a POI together with its interaction partners.

As our light-controlled purification approach is characterized by the very mild elution condition (740 nm light), we next asked whether we could use the flow-throughs of the last washing step performed under 660 nm illumination as background control instead of the eluates from the Jurkat cell line (expressing untagged ZAP70). Indeed, using this procedure we could identify

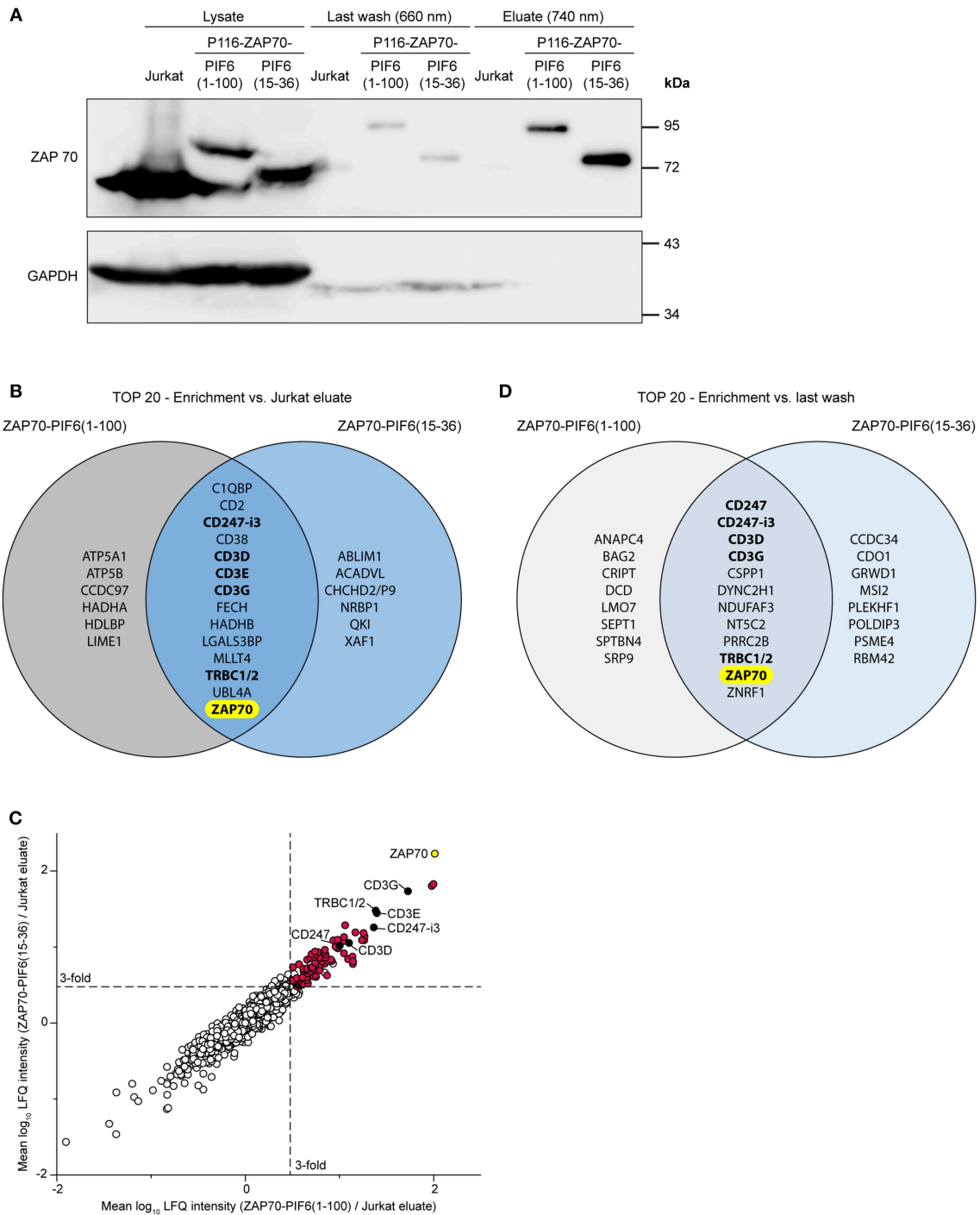


FIGURE 5 | Analysis of light-controlled ZAP70-PIF purification by mass spectrometry. Jurkat cells and P116-derived cell lines stably expressing ZAP70-PIF6(1-100) or ZAP70-PIF6(15-36) were lysed and PIF-tagged proteins were light-controlled purified using PhyB^{*} beads ($n = 3$ biological replicates). All eluates and the flow-throughs of the last washing were analyzed by mass spectrometry. **(A)** Analysis of the cell lysates, the flow-throughs of the last washing step and the eluates by SDS-PAGE and Western blot against ZAP70 and GAPDH. **(B)** Comparison of the 20 best hits ($p < 0.05$, sorted on protein enrichment) enriched in the eluates of each ZAP70-PIF6 cell line vs. the eluates from the Jurkat cell line. Known interaction partners of ZAP70 are written in bold. **(C)** Enrichment of proteins identified in the ZAP70-PIF6(1-100) eluate vs. the Jurkat eluate (x-axis) plotted against the enrichment of proteins in the ZAP70-PIF6(15-36) eluate vs. the Jurkat eluate (y-axis). The enrichment for each protein is shown as the mean \log_{10} ratio of the label-free quantification (LFQ) intensities (3 biological replicates) of the compared samples. Known interaction partners of ZAP70 identified in **(B)** are highlighted in black and are labeled. All significant hits ($p < 0.05$) in the upper right quadrant are highlighted in red. The POI ZAP70 is highlighted in yellow. Dashed lines represent a ratio cut-off corresponding to a 3-fold enrichment compared to the Jurkat eluate. **(D)** Comparison of the 20 best hits ($p < 0.05$, sorted on protein enrichment) enriched in the eluates of each ZAP70-PIF6 cell line vs. the flow-throughs of the last washing step. Known interaction partners of ZAP70 are written in bold. CHCHD2/P9, CHCHD2, CHCHD2P9; CD247-i3, CD247 isoform 3; TRBC1/2, TRBC1, TRBC2.

a similar enrichment of ZAP70 for both PIF6 tags and the known interaction partners CD247, CD247-i3, CD3D, CD3G, and TRBC1/2 within the 20 best hits ($p < 0.05$, sorted on protein enrichment, **Figure 5D**). Therefore, the flow-throughs of the last washing step offer an alternative as control to filter out unspecific and false positive proteins.

Finally, we asked whether we could combine the Jurkat eluates and the flow-throughs of the last washing step to confine the interaction partner analysis to the most relevant hits. To this end, we compared for each PIF6 tag separately the 20 best hits ($p < 0.05$, sorted on protein enrichment) enriched in the eluates compared to the Jurkat eluates and to the flow-throughs of the last washing step (**Figure 6, Supplementary Tables 3, 4**). Identical for both PIF6 tags only ZAP70 and the known interaction partners CD247-i3, CD3D, CD3G, TRBC1/2 were overlapping. This suggests that the other proteins were indeed false positives that we were able to filter out. Of note, CD3E was classified as a false positive although it is a known component of the TCR and thus an interaction partner of ZAP70. Together our data suggest that the combined usage of the Jurkat eluates and the flow-throughs of the last washing step as controls can be used to confine the identified proteins to true interaction partners eliminating false positives.

CONCLUSION

In this study we established an optogenetics-based light-controlled affinity purification method making use of the plant PhyB/PIF system. The POI-PIF6 fusion protein is recombinantly produced and bound to a PhyB* resin. It is eluted after affinity purification by changing the wavelength of light from 660 to 740 nm. Compared to other affinity purification methods (see introduction), in which the biochemical or biophysical properties of the elution buffer are changed compared to the washing buffers, light in the red spectrum at the used low intensities is a mild elution condition. Thus, we can reduce the identification of false positives, especially if one uses two controls, namely the flow-through of the last washing step and control cells expressing the untagged POI.

The fast kinetics of the binding and dissociation of the PhyB/PIF system enable to conduct the affinity purification within a short time window, which is beneficial for the investigation of transient and weak interactions. Finally, we reduced the size of the PhyB-interacting fragment of PIF6 from 100 amino acids [PIF6(1-100)] to 22 amino acids [PIF6(15-36)]. The size reduction of the PIF6 tag increases its suitability as affinity tag by decreasing the probability to interfere with the function of the POI and to interact with other proteins. Furthermore, the 22 amino acids PIF6 fragment might also allow novel optogenetic applications using the PhyB/PIF system (19, 32).

MATERIALS AND METHODS

Construction of Plasmids

The design and construction of the plasmids generated in this study are described in **Supplementary Table 5**

and the oligonucleotides used for this purpose in **Supplementary Table 6**. DNA-fragments were amplified by polymerase chain reaction and assembled by an isothermal, enzymatic DNA assembly reaction as described previously (Gibson cloning) (33).

Production of PhyB* and Protein Quantification

PhyB* encoded by plasmid pMH17 was expressed in *E. coli* together with the biosynthesis genes for phycocyanobilin (PCB) encoded by plasmid p171 and purified by immobilized metal ion affinity chromatography (IMAC) as described previously (24). The fluorescent protein GFP-PIF6(1-100)-His₆ encoded by plasmid pHB111 was used as fluorescence standard and was produced in *E. coli* and purified by IMAC as described previously (34). The protein concentrations of the purified proteins were determined by Bradford assay (Bio-Rad, Hercules, CA, cat. no. 500-0006) using bovine serum albumin (BSA, Sigma-Aldrich, St. Louis, MO, cat. no. 05479) as standard.

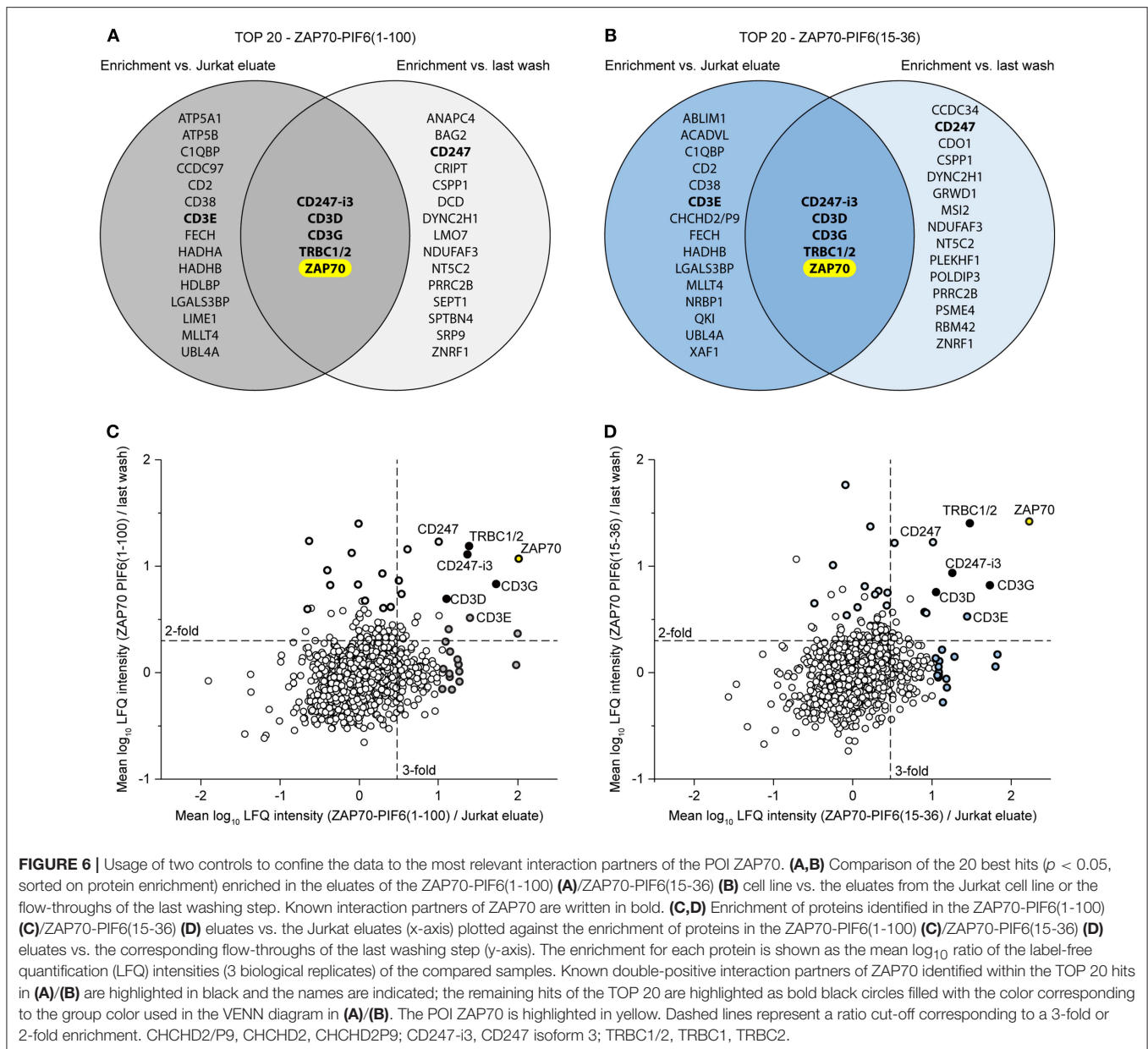
The fluorescent proteins GFP and mCherry were quantified by measuring their fluorescence (GFP: excitation: 488 nm, emission: 522 nm; mCherry: excitation: 588 nm, emission: 620 nm) with an Infinite M200 Pro microplate reader (Tecan, Männedorf, Switzerland). The concentration of all GFP-containing proteins expressed in HEK-293T cells was calculated based on the fluorescence using purified GFP-PIF6(1-100)-His₆ in wash buffer [20 mM Tris/HCl, 137 mM NaCl, 2 mM EDTA, 10% (v/v) glycerol, pH 7.4] as standard. In **Supplementary Figure 1**, the concentration of unbound PhyB* was determined by measuring PhyB* fluorescence (excitation: 620 nm, emission: 680 nm) after 660 nm illumination (10 min, 20 $\mu\text{mol m}^{-2} \text{s}^{-1}$) with an Infinite M200 Pro microplate reader.

Maintenance of Mammalian Cells

HEK-293T cells were maintained in DMEM complete medium [DMEM (PAN Biotech, Aidenbach, Germany, cat. no. P04-03550), 10% (v/v) fetal calf serum (FCS, PAN Biotech, cat. no. P30-3602), 100 U ml⁻¹ penicillin, 100 $\mu\text{g ml}^{-1}$ streptomycin]. Jurkat, P116 (27) and transduced P116 cells were cultivated in RPMI complete medium [RPMI 1640 (Thermo Fisher Scientific, Waltham, MA, cat. no. 31870-025), 10% (v/v) FCS (PeproTech, Hamburg, Germany, cat. no. 200-02), 2 mM L-glutamine, 100 U ml⁻¹ penicillin, 100 $\mu\text{g ml}^{-1}$ streptomycin, 10 mM HEPES (Thermo Fisher Scientific, cat. no. 15630-056)]. All cells were incubated in a humidified atmosphere at 37°C, 5% CO₂.

Expression and Harvesting of GFP Fused to Different Affinity Tags

All constructs encoding untagged mCherry and GFP fused to different affinity tags (**Figure 2A, Supplementary Table 5**) were expressed in HEK-293T cells. To this aim, 6×10^6 HEK-293T cells were seeded per 15 cm culture dish and transfected 24 h later with the corresponding plasmid. Per 15 cm dish, 60 μg plasmid DNA, and 200 μg PEI (linear, MW: 25 kDa, Polysciences, Warrington, PA, cat. no. 23966-2) were mixed in 3 ml OptiMEM (Thermo Fisher Scientific, cat. no. 22600-134), incubated for 15 min at RT and added dropwise to the



cells. After incubation for 5 h, the medium was exchanged and proteins were expressed for 48 h. Before harvesting, the cells were washed once with DBPS containing Ca^{2+} and Mg^{2+} (PAN Biotech, cat. no. P04-35500) and cells were lysed—if not stated otherwise—with 3 ml of lysis buffer [20 mM Tris/HCl, 137 mM NaCl, 2 mM EDTA, 10% (v/v) glycerol, pH 7.4, protease inhibitor cocktail (Sigma-Aldrich, cat. no. SRE0055), 0.5% (v/v) Brij97 (Sigma-Aldrich, cat. no. 431281-100ML)] per 15 cm culture dish for 20 min on ice. After clarifying the lysate by centrifugation at $16,500 \times g$ for 15 min, the supernatant was either immediately further processed or shock-frozen in liquid nitrogen and stored at -80°C . The average yield of GFP-PIF6(1-100) was $\sim 720 \mu\text{g}$ of purified protein per 15 cm dish.

Light-Controlled Affinity Purification

NeutrAvidin agarose beads (Thermo Fisher Scientific, cat. no. 29202) were washed once with Ni-Elution buffer (50 mM NaH_2PO_4 , 300 mM NaCl, 250 mM imidazole, pH 8.0) and incubated afterwards with purified PhyB* in Ni-Elution buffer supplemented with 1 mM 2-mercaptoethanol (final PhyB* concentration: $\sim 2 \text{ mg ml}^{-1}$) for 2 h at 4°C under slight agitation. If not otherwise stated, $1 \mu\text{l}$ NeutrAvidin beads were incubated with 0.27 nmol PhyB*. After washing the beads twice with wash buffer, the beads were resuspended in lysis buffer and the indicated amounts of beads were transferred into a spin column (Thermo Fisher Scientific, cat. no. 69725). Subsequently, the cell lysate was added to the beads and the closed spin column was incubated on a rotator for 60 min under 660 nm illumination

(10 $\mu\text{mol m}^{-2} \text{s}^{-1}$) at 4°C. All following steps were performed under green safe light at 4°C. After incubation, the beads were washed by centrifugation of the spin column at 150 \times g for 30 s, addition of 500 μl of wash buffer and incubation of the closed spin column for 10 min on a rotator under 660 nm illumination. This washing step was repeated for the indicated number of times (3 \times if not indicated otherwise). Afterwards, the column was centrifuged before 500 μl of wash buffer were added and the column was incubated under 740 nm light (70 $\mu\text{mol m}^{-2} \text{s}^{-1}$) on a rotator for 10 min. Finally, the eluted proteins were collected by centrifugation of the spin column.

Affinity Purification of GFP With SBP Tag

The indicated number of HEK-293T cells transfected with plasmid pMH501 (as described above) were lysed 48 h after transfection with 500 μl of lysis buffer. All following steps were performed at 4°C. The soluble fraction of the cell lysate was incubated with the indicated amount of prewashed streptavidin Sepharose beads (GE Healthcare, Freiburg, Germany, cat. no. 17-5113-01) within a closed spin column on a rotator at 4°C for 2 h. Afterwards, the beads were washed by centrifugation (150 \times g, 30 s) of the column, addition of 500 μl of wash buffer and incubation of the closed spin column for 10 min on a rotator. After repeating this washing step for three times, the column was centrifuged and 500 μl of elution buffer (wash buffer supplemented with 2 mM biotin) was added and the closed spin column was incubated on a rotator at 4°C for 20 min. Finally, the eluted proteins were collected by centrifugation.

Affinity Purification of GFP With TEV_{CS}-ProteinA Tag

The indicated number of HEK-293T cells transfected with plasmid pMH502 (as described above) were lysed 48 h after transfection with 500 μl of lysis buffer. All following steps were performed at 4°C. The soluble fraction of the lysate was incubated with the indicated amount of prewashed IgG Sepharose beads (35) within a closed spin column (Mobicol Classic with 35 μm pore size filter, MoBiTec, Göttingen, Germany, cat. no. M1003 and M513515) on a rotator at 4°C overnight. Afterwards, the beads were washed by centrifugation (150 \times g, 30 s) of the column, addition of 500 μl of wash buffer and incubation of the closed spin column for 10 min on a rotator. After repeating this washing step three times, the columns were centrifuged and the beads were resuspended in 500 μl of wash buffer containing TEV protease (1 U TEV per 1 μl of beads, Thermo Fisher Scientific, cat. no. 12575015). After incubation on a shaker at 16°C for 3 h, prewashed Ni-NTA agarose beads (1 μl Ni-NTA beads per 2 μl of IgG beads) were added to remove the His₆-tagged TEV protease and the sample was incubated for further 2 h. Finally, the eluted proteins were collected by centrifugation.

Generation of Stable Cell Lines

The P116-based cell lines stably expressing ZAP70-PIF6(1-100) or ZAP70-PIF6(15-36) were generated by transduction with lentiviral particles. For lentiviral particle production, 8 \times 10⁶ HEK293-T cells were seeded in DMEM lenti [Advanced

DMEM (Thermo Fisher Scientific, cat. no. 12491015), 2% (v/v) FCS, 100 U ml⁻¹ penicillin, and 100 $\mu\text{g ml}^{-1}$ streptomycin, 10 μM cholesterol, 10 μM egg lecithin (Serva Electrophoresis, Heidelberg, Germany, cat. no. 27608), 1 \times chemical defined lipid concentrate (Thermo Fisher Scientific, cat. no. 11905031)] per 15 cm dish. On the next day, the cells were transfected as described above with the plasmids pMH511 or pMH521, pLTR-G (36), and pCD/NL-BH* $\Delta\Delta\Delta$ (37) in a mass ratio of 2:1:1 and the medium was replaced after 5 h with fresh DMEM lenti. After 48 h, the supernatant containing the lentiviral particle was harvested and filtered through a 0.45 μm filter. For transduction, P116 cells at a density of 3 \times 10⁵ cells ml⁻¹ were diluted 1:2 with the filtered lentiviral particle-containing supernatant. After 96 h, cells with low expression of the fluorescent protein ZsGreen1 were sorted using an S3e Cell Sorter (Bio-Rad).

Lysis of T Cells

For Western blot analysis (Figure 4C) and for each mass spectrometry measurement, 1 \times 10⁶ or 250 \times 10⁶ cells were resuspended in 50 or 500 μl of lysis buffer supplemented with 1 mM phenylmethylsulfonyl fluoride, 5 mM iodoacetamide, 0.5 mM sodium orthovanadate, and 1 mM NaF, respectively. After incubation for 15 min on ice the lysate was clarified by centrifugation for 15 min at 16,500 \times g. The supernatant was either mixed with SDS loading buffer for Western Blot analysis or used for light-controlled affinity purification (200 μl of PhyB* beads, four washing steps) and subsequent mass spectrometry analysis.

Western Blots

For Western blots, proteins were transferred after SDS-PAGE onto PVDF membranes and the membranes were blocked with TBS-T [TBS (50 mM Tris/HCl, 150 mM NaCl, pH 7.4) with 0.05% (v/v) Tween-20] containing 5% (w/v) milk powder for 1 h at RT. Afterwards, the membranes were incubated with the primary antibody (anti-ZAP70, dilution: 1:500, Santa Cruz Biotechnology, Dallas, TX, cat. no. sc-30674 or anti-GAPDH, dilution: 1:100,000, Cell Signaling, Danvers, MA, cat. no. 5174) diluted in TBS-T supplemented with 3% (w/v) BSA and 0.02% (w/v) sodium azide at 4°C overnight. After washing the membrane three times with TBS-T, they were incubated with the secondary antibody (ZAP70: rabbit anti-goat IgG-HRP, dilution: 1:10,000, Thermo Fisher Scientific, cat. no. 31402 or GAPDH: goat anti-rabbit IgG-HRP, dilution: 1:10,000, Thermo Fisher Scientific, cat. no. 31460) diluted in TBS-T supplemented with 3% (w/v) BSA and 3% (w/v) milk powder for 1 h at RT. Following three washing steps with TBS-T, chemiluminescence was detected using ECL substrate and an ImageQuant LAS-4000 mini system (GE Healthcare).

Ca²⁺-Flux Measurements

For measuring of Ca²⁺-flux, 5 \times 10⁶ cells were washed with PBS and incubated in 1 ml starvation medium (RPMI complete containing 1% (v/v) FCS) containing 4 μM Indo-1 (Thermo Fisher Scientific, cat. no. I1223) and 0.1% (v/v) Pluronic F-127 (Thermo Fisher Scientific, cat. no. P3000MP) for 1 h at 37°C, 5% CO₂. Afterwards, the cells were pelleted by centrifugation,

resuspended in 500 μl of starvation medium and kept on ice in the dark until the measurement. Analyses of Ca^{2+} -bound and unbound Indo-1 was performed with a customized MACSQuant Analyzer (Miltenyi Biotec, Bergisch Gladbach, Germany) using a 355 nm laser and 405/20 nm and 530/30 nm emission filters, respectively. Cells were stimulated with 1 $\mu\text{g ml}^{-1}$ anti-CD3 antibody (UCHT1, Dr. Beverly, UK).

Mass Spectrometry

The proteins present within 400 μl of the sample (either eluate or flow-through of the last washing step from the light-controlled affinity purification) were precipitated by addition of 1.6 ml of ice-cold acetone and incubation at -20°C overnight. Afterwards, the precipitated proteins were pelleted by centrifugation at $10,000 \times g$ for 10 min at 4°C and the air-dried pellet was resolubilized in 10 μl of buffer (60% (v/v) methanol in 50 mM NH_4HCO_3). The disulfide bonds were then reduced with 5 mM tris(2-carboxyethyl)phosphine (TCEP) for 30 min at 65°C , and afterwards alkylated with 50 mM 2-chloroacetamide for 30 min at RT. The reaction was quenched by addition of 25 mM dithiothreitol (DTT), diluted with 25 μl buffer and the proteins were digested with 1 μg trypsin (Promega, Mannheim Germany, cat. no. V5111) at 42°C for 4 h. The samples were dried in a vacuum concentrator and resuspended in 15 μl of 0.1% (v/v) trifluoroacetic acid (TFA) prior to mass spectrometry (MS) analysis.

Liquid chromatography-tandem mass spectrometry (LC-MS/MS) analysis was performed with an UltiMate 3000 RLSCnano HPLC System (Thermo Fisher Scientific) coupled online to a Q Exactive Plus instrument (Thermo Fisher Scientific) essentially as described previously (38). Samples were washed on a C18 pre-column (Ø 0.3 \times 5 mm; PepMap, Thermo Fisher Scientific) using 0.1% (v/v) TFA for 15 min, which was thereafter switched in line with the analytical column (Acclaim PepMap (ID: 75 μm \times 250 mm, 2 μm , 100 Å , Dionex LC Packings/Thermo Fisher Scientific), equilibrated in 96% solvent A [0.1% (v/v) formic acid (FA)] and 4% solvent B (0.1% (v/v) FA, 86% (v/v) CH_3CN). A gradient of 100 min (4–40% solvent B in 95 min and 40–95% solvent B in 5 min) at a flow rate of 0.250 $\mu\text{l min}^{-1}$ was applied to separate the peptide mixture. The column was washed for 5 min with 95% solvent B, before re-equilibration for 15 min. The Q Exactive Plus acquired mass spectra from m/z 375 to 1,700, with a resolution of 70,000 at m/z 200 [parameters: automatic gain control (AGC), 3×10^6 ions; maximum fill time, 60 ms]. The instrument operated in the data-dependent mode, using a TOP 15 method for the isolation of precursor ions (parameters: AGC target, 1×10^5 ions; fill time, 120 ms; isolation window, 3 m/z ; normalized collision energy, 28; underfill ratio, 1.2%; dynamic exclusion, 45 s).

Mass Spectrometry Data Analysis

For mass spectrometry data analysis, MaxQuant version 1.5.5.1 with its integrated search engine Andromeda was used to search peak lists against the Uniprot proteome set *H. sapiens* (database 19/09/2018, 95109 entries) (39, 40). The search was conducted with default parameters (e.g., FDR 1% on protein and peptide level; precursor mass tolerance 20 ppm for the first search, 4.5 ppm for the main search), except the

following adjustments: trypsin was selected as proteolytic enzyme and up to three missed cleavages were allowed. As variable modifications oxidation on methionine and acetylation on protein N-termini were selected. Cysteine carbamidomethylation was set as fixed modification. Protein identification required at least one unique peptide. Label-free quantification (LFQ) (41) was enabled, the LFQ minimal ratio count was set to 2 and fast LFQ was disabled. “Match between runs” was enabled with default parameters.

The LFQ intensities from the proteingroups.txt output file of MaxQuant were loaded into Perseus version 1.5.5.3 (42). Entries from contaminants, reverse hits and hits only identified by modified peptides were discarded. LFQ intensities were \log_{10} -transformed and proteingroups with 3 out of 3 valid values (3 independent biological replicates) in the ZAP70-PIF pulldown samples were used for further data analysis. Subsequently, for missing values of the control and wash samples random numbers were imputed from normal distribution (width of the distribution 0.5, down shift 1.8) to simulate values below the detection limit. To identify significantly enriched proteins, a right-sided, two-sample *t*-test was performed. Results were imported into Origin Pro 2017 (OriginLab, Northampton, MA) and visualized as scatter plots.

DATA AVAILABILITY

The mass spectrometry proteomics data have been deposited to the ProteomeXchange Consortium via the PRIDE (43) partner repository with the dataset identifier PXD012156. All other raw data supporting the conclusions of this manuscript will be made available by the authors, without undue reservation, to any qualified researcher.

AUTHOR CONTRIBUTIONS

MH and JE planned and performed all experiments to set up the new purification protocol, and MH, OY, and JE the ones involving the P116T cells. JS performed interactome studies by LC-MS followed by quantitative data analysis. MH, OY, BW, WW, and WS were involved in the design, supervision, and analysis of all experiments. MH, JE, and WS wrote the manuscript with input from all authors.

FUNDING

This work was funded by the German Research Foundation (DFG) under the Excellence Initiative (BIOSS - EXC-294 (to WW, WS, and BW) and SGBM - GSC-4 (to MH, OY, and JS)) and the Excellence Strategy (CIBSS - EXC-2189 - Project ID 390939984) to WW, WS, and BW as well as through the collaborative research center DFG-TRR 130 to BW.

SUPPLEMENTARY MATERIAL

The Supplementary Material for this article can be found online at: <https://www.frontiersin.org/articles/10.3389/fimmu.2019.00226/full#supplementary-material>

REFERENCES

- Krogan NJ, Cagney G, Yu H, Zhong G, Guo X, Ignatchenko A, et al. Global landscape of protein complexes in the yeast *Saccharomyces cerevisiae*. *Nature* (2006) 440:637–43. doi: 10.1038/nature04670
- Huttlin EL, Bruckner RJ, Paulo JA, Cannon JR, Ting L, Baltier K, et al. Architecture of the human interactome defines protein communities and disease networks. *Nature* (2017) 545:505–9. doi: 10.1038/nature22366
- Balogopalan L, Kortum RL, Coussens NP, Barr VA, Samelson LE. The linker for activation of T cells (LAT) signaling hub: from signaling complexes to microclusters. *J Biol Chem.* (2015) 290:26422–9. doi: 10.1074/jbc.R115.665869
- Lork M, Staal J, Beyaert R. Ubiquitination and phosphorylation of the CARD11-BCL10-MALT1 signalosome in T cells. *Cell Immunol.* (2018) doi: 10.1016/j.cellimm.2018.11.001. [Epub ahead of print].
- Chan AC, Iwashima M, Turck CW, Weiss A. Zap-70 - a 70 Kd protein-tyrosine kinase that associates with the Tcr Zeta-Chain. *Cell* (1992) 71:649–62. doi: 10.1016/0092-8674(92)90598-7
- Iwashima M, Irving BA, van Oers NS, Chan AC, Weiss A. Sequential interactions of the TCR with two distinct cytoplasmic tyrosine kinases. *Science* (1994) 263:1136–9. doi: 10.1126/science.7509083
- van Oers NSC, Killeen N, Weiss A. Zap-70 is constitutively associated with tyrosine-phosphorylated tcr-Zeta in murine thymocytes and lymph-node T-cells. *Immunity* (1994) 1:675–85. doi: 10.1016/1074-7613(94)90038-8
- Au-Yeung BB, Deindl S, Hsu LY, Palacios EH, Levin SE, Kuriyan J, et al. The structure, regulation, and function of ZAP-70. *Immunol Rev.* (2009) 228:41–57. doi: 10.1111/j.1600-065X.2008.00753.x
- Katz ZB, Novotna L, Blount A, Lillemeier BF. A cycle of Zap70 kinase activation and release from the TCR amplifies and disperses antigenic stimuli. *Nat Immunol.* (2017) 18:86–95. doi: 10.1038/ni.3631
- Roncagalli R, Hauri S, Fiore F, Liang Y, Chen Z, Sansoni A, et al. Quantitative proteomics analysis of signalosome dynamics in primary T cells identifies the surface receptor CD6 as a Lat adaptor-independent TCR signaling hub. *Nat Immunol.* (2014) 15:384–92. doi: 10.1038/ni.2843
- Gingras AC, Gstaiger M, Raught B, Aebersold R. Analysis of protein complexes using mass spectrometry. *Nat Rev Mol Cell Biol.* (2007) 8:645–54. doi: 10.1038/nrm2208
- Pardo M, Choudhary JS. Assignment of protein interactions from affinity purification/mass spectrometry data. *J Proteome Res.* (2012) 11:1462–74. doi: 10.1021/pr2011632
- Terpe K. Overview of tag protein fusions: from molecular and biochemical fundamentals to commercial systems. *Appl Microbiol Biotechnol.* (2003) 60:523–33. doi: 10.1007/s00253-002-1158-6
- Pina AS, Lowe CR, Roque AC. Challenges and opportunities in the purification of recombinant tagged proteins. *Biotechnol Adv.* (2014) 32:366–81. doi: 10.1016/j.biotechadv.2013.12.001
- Parks TD, Leuther KK, Howard ED, Johnston SA, Dougherty WG. Release of proteins and peptides from fusion proteins using a recombinant plant-virus proteinase. *Anal Biochem.* (1994) 216:413–7. doi: 10.1006/abio.1994.1060
- Rigaut G, Shevchenko A, Rutz B, Wilm M, Mann M, Seraphin B. A generic protein purification method for protein complex characterization and proteome exploration. *Nat Biotechnol.* (1999) 17:1030–2. doi: 10.1038/13732
- Khanna R, Huq E, Kikis EA, Al-Sady B, Lanzatella C, Quail PH. A novel molecular recognition motif necessary for targeting photoactivated phytochrome signaling to specific basic helix-loop-helix transcription factors. *Plant Cell* (2004) 16:3033–44. doi: 10.1105/tpc.104.025643
- Levskaya A, Weiner OD, Lim WA, Voigt CA. Spatiotemporal control of cell signalling using a light-switchable protein interaction. *Nature* (2009) 461:997–1001. doi: 10.1038/nature08446
- Kolar K, Knobloch C, Stork H, Znidaric M, Weber W. OptoBase: a web platform for molecular optogenetics. *ACS Synth Biol.* (2018) 7:1825–8. doi: 10.1021/acssynbio.8b00120
- Adrian M, Nijenhuis W, Hoogstraaten RI, Willems J, Kapitein LC. A phytochrome-derived photoswitch for intracellular transport. *ACS Synth Biol.* (2017) 6:1248–56. doi: 10.1021/acssynbio.6b00333
- Toettcher JE, Weiner OD, Lim WA. Using optogenetics to interrogate the dynamic control of signal transmission by the ras/erk module. *Cell* (2013) 155:1422–34. doi: 10.1016/j.cell.2013.11.004
- Beyer HM, Juillot S, Herbst K, Samodelov SL, Müller K, Schamel WW, et al. Red light-regulated reversible nuclear localization of proteins in mammalian cells and zebrafish. *ACS Synth Biol.* (2015) 4:951–8. doi: 10.1021/acssynbio.5b00004
- Müller K, Engesser R, Metzger S, Schulz S, Kämpf MM, Busacker M, et al. A red/far-red light-responsive bi-stable toggle switch to control gene expression in mammalian cells. *Nucleic Acids Res.* (2013) 41:e77. doi: 10.1093/nar/gkt002
- Smith RW, Helwig B, Westphal AH, Pel E, Hörner M, Beyer HM, et al. Unearthing the transition rates between photoreceptor conformers. *BMC Syst Biol.* (2016) 10:110. doi: 10.1186/s12918-016-0368-y
- Keefe AD, Wilson DS, Seelig B, Szostak JW. One-step purification of recombinant proteins using a nanomolar-affinity streptavidin-binding peptide, the SBP-tag. *Protein Expr Purif.* (2001) 23:440–6. doi: 10.1006/prep.2001.1515
- Knop M, Siegers K, Pereira G, Zachariae W, Winsor B, Nasmyth K, et al. Epitope tagging of yeast genes using a PCR-based strategy: more tags and improved practical routines. *Yeast* (1999) 15:963–72. doi: 10.1002/(Sici)1097-0061(199907)15:10b<963::Aid-Yea399>3.0.Co;2-W
- Williams BL, Schreiber KL, Zhang W, Wange RL, Samelson LE, Leibson PJ, et al. Genetic evidence for differential coupling of Syk family kinases to the T-cell receptor: reconstitution studies in a ZAP-70-deficient Jurkat T-cell line. *Mol Cell Biol.* (1998) 18:1388–99. doi: 10.1128/MCB.18.3.1388
- Schamel WW, Alarcon B. Organization of the resting TCR in nanoscale oligomers. *Immunol Rev.* (2013) 251:13–20. doi: 10.1111/imr.12019
- Weiss A, Littman DR. Signal transduction by lymphocyte antigen receptors. *Cell* (1994) 76:263–74. doi: 10.1016/0092-8674(94)90334-4
- Qian DP, Mollenauer MN, Weiss A. Dominant-negative zeta-associated protein 70 inhibits T cell antigen receptor signaling. *J Exp Med.* (1996) 183:611–20. doi: 10.1084/jem.183.2.611
- Roose JP, Diehn M, Tomlinson MG, Lin J, Alizadeh AA, Botstein D, et al. T cell receptor-independent basal signaling via Erk and Abl kinases suppresses RAG gene expression. *PLoS Biol.* (2003) 1:271–87. doi: 10.1371/journal.pbio.0000053
- Tischer D, Weiner OD. Illuminating cell signalling with optogenetic tools. *Nat Rev Mol Cell Biol.* (2014) 15:551–8. doi: 10.1038/nrm3837
- Gibson DG, Young L, Chuang RY, Venter JC, Hutchison CA III, Smith HO. Enzymatic assembly of DNA molecules up to several hundred kilobases. *Nat. Methods* (2009) 6:343–5. doi: 10.1038/nmeth.1318
- Beyer HM, Thomas OS, Riegel N, Zurbriggen MD, Weber W, Hörner M. Generic and reversible opto-trapping of biomolecules. *Acta Biomater.* (2018) 79:276–82. doi: 10.1016/j.actbio.2018.08.032
- Piechura H, Oeljeklaus S, Warscheid B. SILAC for the study of mammalian cell lines and yeast protein complexes. *Methods Mol Biol.* (2012) 893:201–21. doi: 10.1007/978-1-61779-885-6_14
- Reiser J, Harmison G, Kluepfel-Stahl S, Brady RO, Karlsson S, Schubert M. Transduction of nondividing cells using pseudotyped defective high-titer HIV type 1 particles. *Proc Natl Acad Sci USA.* (1996) 93:15266–71.
- Zhang XY, La Russa VF, Reiser J. Transduction of bone-marrow-derived mesenchymal stem cells by using lentivirus vectors pseudotyped with modified RD114 envelope glycoproteins. *J Virol.* (2004) 78:1219–29. doi: 10.1128/JVI.78.3.1219-1229.2004
- Reimann L, Wiese H, Leber Y, Schwable AN, Fricke AL, Rohland A, et al. Myofibrillar Z-discs are a protein phosphorylation hot spot with protein kinase C (PKC α) modulating protein dynamics. *Mol Cell Proteomics* (2017) 16:346–67. doi: 10.1074/mcp.M116.065425

39. Cox J, Mann M. MaxQuant enables high peptide identification rates, individualized p.p.b.-range mass accuracies and proteome-wide protein quantification. *Nat Biotechnol.* (2008) 26:1367–72. doi: 10.1038/nbt.1511
40. Cox J, Neuhauser N, Michalski A, Scheltema RA, Olsen JV, Mann M. Andromeda: a peptide search engine integrated into the maxquant environment. *J Proteome Res.* (2011) 10:1794–805. doi: 10.1021/pr101065j
41. Cox J, Hein MY, Lubner CA, Paron I, Nagaraj N, Mann M. Accurate proteome-wide label-free quantification by delayed normalization and maximal peptide ratio extraction, termed MaxLFQ. *Mol Cell Proteomics* (2014) 13:2513–26. doi: 10.1074/mcp.M113.031591
42. Tyanova S, Temu T, Sinitcyn P, Carlson A, Hein MY, Geiger T, et al. The perseus computational platform for comprehensive analysis of (prote)omics data. *Nat Methods* (2016) 13:731–40. doi: 10.1038/Nmeth.3901
43. Vizcaino JA, Csordas A, Del-Toro N, Dianas JA, Griss J, Lavidas I, et al. 2016 update of the PRIDE database and its related tools. *Nucleic Acids Res.* (2016) 44:D447–56. doi: 10.1093/nar/gkw880

Conflict of Interest Statement: The authors declare that the research was conducted in the absence of any commercial or financial relationships that could be construed as a potential conflict of interest.

Copyright © 2019 Hörner, Eble, Yousefi, Schwarz, Warscheid, Weber and Schamel. This is an open-access article distributed under the terms of the Creative Commons Attribution License (CC BY). The use, distribution or reproduction in other forums is permitted, provided the original author(s) and the copyright owner(s) are credited and that the original publication in this journal is cited, in accordance with accepted academic practice. No use, distribution or reproduction is permitted which does not comply with these terms.